

## The effects of additive noise and drift in the dynamics of the driving on chaotic synchronization

Reggie Brown<sup>a</sup>, Nikolai F. Rulkov<sup>a</sup>, Nicholas B. Tufillaro<sup>b</sup>

<sup>a</sup> Institute for Nonlinear Science, University of California, San Diego, La Jolla, CA 92093-0402, USA

<sup>b</sup> Center for Nonlinear Studies, Los Alamos National Laboratory, Los Alamos, NM 87545, USA

Received 27 May 1994; revised manuscript received 28 October 1994; accepted for publication 1 November 1994

Communicated by A.R. Bishop

---

### Abstract

We examine the effect of additive noise in, and drift in the dynamics of, a chaotic driving signal on the synchronization of chaotic response systems. Simple scaling laws associated with the synchronization deviation level under these types of contamination are presented. Time series used as the driving signals are experimentally measured from an electronic circuit.

---

Synchronization between two chaotic systems has received considerable attention in recent years. Most of this work has been associated with identical, chaotic in time, behavior brought about by coupling two or more identical systems in a drive/response manner [1]. (Other useful references are, and can be found in, Refs. [2–4].) Unless otherwise specified synchronization will mean this form of identical synchronous motion of identical systems.

This Letter examines the following questions regarding the appearance of deviations from identical synchronous motion: (1) How will additive noise in the driving signal affect synchronization? (2) How will small differences between the dynamics of the driving and response systems affect synchronization? Similar questions have been addressed by others [5,6]. Suggested applications for synchronization involve communications [7–9], nondestructive testing, failure monitoring, and system identification [3]. The two questions we address are important to these applications.

Our research uses numerical models constructed

from experimentally measured time series data as the response system [10]. Time series measurements are also used as the driving system. The “working phase space” is the one where the global dynamics is being modeled [4,11] and is typically a  $d$ -dimensional Euclidean space. In the working phase space, let the unknown dynamics of the driving system and the known dynamics of the model be represented by

$$\frac{dx}{dt} = G(x) \quad (1)$$

and

$$\frac{dx}{dt} = F(x), \quad (2)$$

respectively. The only thing known, a priori, about  $G$  are time series measurements.

In the working phase space an experimentally measured driving signal,  $x + \sigma\hat{u}$ , is the sum of clean dynamics,  $x$ , and measurement noise,  $\sigma\hat{u}$ . We indicate the size of the noise by  $\sigma$  while  $\hat{u}$  is a signal of unit size. Now assume that a model, Eq. (2), has been con-

structed from a time series which is not the same as the driving time series (although they may have the same source) [10,12]. By dissipatively coupling  $F$  to the driving signal via

$$\frac{dy}{dt} = F(y) - E \cdot [y - (x + \sigma \hat{u})], \quad (3)$$

it is possible to almost synchronize  $F$  to  $x$  [5,10,13].

The coupling matrix  $E$  has only one nonzero element,  $E_{\beta\beta} = \epsilon$ , where  $x_\beta + \sigma\eta$  is the  $\beta$  component of the driving signal. If the coupling,  $\epsilon$ , is too small then, clearly, synchronization will not occur. It is also possible that if  $\epsilon$  is too large then synchronization (or almost synchronization) will not occur [5,10,13]. All of our numerical experiments used  $\beta = d$  as the driving term. For the systems we have studied the  $\epsilon \rightarrow \infty$  limit still resulted in near synchronization. Thus, for our numerical experiments noise and errors in modeling are the causes of any lack of complete synchronization.

By definition, the model is synchronized to the time series,  $x$ , if  $x = y$  and  $F = G$  for all time greater than  $t_0$ , a transient. Synchronization will not occur if  $F \neq G$  and/or in the presence of noise [10]. However, if the model is close to the true dynamics and if the noise level is not too large then it is possible for the model to nearly synchronize to the true driving dynamics. To quantify this notion let  $z = y - x$  denote the deviations between  $y$  and the clean driving signal,  $x$ . It has been previously shown that for the systems we are considering  $0 < |z|^2 \ll 1$  and the average value of  $\log_{10}(|z|^2)$  is essentially constant [3,10]. Therefore, it is appropriate to consider the linearized time evolution of  $z$  as given by

$$\frac{dz}{dt} = [DF(x) - E] \cdot z + \sigma E \cdot \hat{u} + \Delta G(x), \quad (4)$$

where  $\Delta G = F - G$  denotes the difference between the model and the true dynamics of the driving system.

$\Delta G$  is not related to measurement errors and has two potential sources. The first source occurs because, for any real situation  $F$  is never *exactly* equal to  $G$ . The second source occurs if the dynamics of the driving signal,  $G$ , is different from the dynamics that produced the time series used to make the model,  $G'$ . To analytically isolate these causes note that if  $G$  and  $G'$  are related by a small change in the parameters of the driving system, then

$$\Delta G(x) \simeq \Delta G'(x) + \left( \frac{\partial}{\partial p} \Delta G'(x) \right) \cdot \delta p, \quad (5)$$

where  $p$  represents the parameters of the system, the change in parameters is small ( $|\delta p| \ll 1$ ), and  $\Delta G' = F - G'$ . The first and second terms on the right hand side of Eq. (5) are associated with modeling errors and drift in the dynamics of the driving system, respectively.

Since the average of  $\log_{10}(|z|^2)$  is essentially constant we define the synchronization deviation level (which we sometimes call the deviation level) by

$$[\langle |z|^2 \rangle_T]^{1/2} = \left( \lim_{t \rightarrow \infty} \frac{1}{t - t_0} \int_{t_0}^t |z(r)|^2 dr \right)^{1/2}. \quad (6)$$

We assume that the noise, and  $\Delta G$ , are ergodic. This allows us to replace time averages by phase space averages (which will be denoted by angular brackets,  $\langle \rangle$ ). We also assume that the noise is stationary and completely independent of  $\Delta G$ . With these assumptions it is possible to rewrite Eq. (6) as [3]

$$[\langle |z|^2 \rangle_T]^{1/2} = [A^2 + (\sigma B)^2]^{1/2}, \quad (7)$$

where  $B^2$  and  $A^2$  are given by

$$B^2 = \epsilon^2 k(0) \left( \int_{t_0}^t \langle |U(t,r) \cdot V|^2 \rangle dr + 2 \int_{t_0}^t \langle [U(t,r) \cdot V] \cdot [U(t,r) \cdot B(r)] \rangle dr \right), \quad (8)$$

$$A^2 = \int_{t_0}^t \langle |U(t,r) \cdot \Delta G(r)|^2 \rangle dr + 2 \int_{t_0}^t \langle [U(t,r) \cdot \Delta G(r)] \cdot [U(t,r) \cdot H(r)] \rangle dr, \quad (9)$$

and  $k(s)$  is the autocorrelation function of the noise.

The  $d$ -dimensional vectors,  $V$ ,  $B(r) = B[x(r)]$ , and  $H(r) = H[x(r)]$  are defined in the following manner.  $V = [0, \dots, 0, 1, 0, \dots, 0]$  where the 1 appears as the  $\beta$  element of  $V$  if  $\beta$  is the component of  $x$  used as the drive signal.  $B(r)$  and  $H(r)$  are defined by

$$\mathbf{B}(r) = \int_{0^+}^r \frac{k(s)}{k(0)} \mathbf{U}(r, r-s) \cdot \mathbf{V} ds,$$

$$\mathbf{H}(r) = \int_{0^+}^r \mathbf{U}(r, r-s) \cdot \Delta \mathbf{G}(r-s) ds,$$

where  $\Delta \mathbf{G}(r) = \Delta \mathbf{G}[\mathbf{x}(r)]$ . The lower limit of integration,  $0^+$ , implies taking the limit as we approach, but are never equal to, 0 from the positive side.

The matrix  $\mathbf{U}(t, t_0)$  satisfies the initial condition  $\mathbf{U}(t_0, t_0) = \mathbf{1}$  (where  $\mathbf{1}$  is the identity) and is the evolution operator that evolve  $\mathbf{z}(t_0)$ , forward in time from  $t_0$  to  $t$  in the presence of coupling and the absence of noise and modeling errors. It comes from the solution to the homogeneous portion of Eq. (4) and is defined by

$$\begin{aligned} \mathbf{z}(t) &= \exp \left( \int_{t_0}^t [\mathbf{D}\mathbf{F}(r) - \mathbf{E}] dr \right) \cdot \mathbf{z}(t_0) \\ &= \mathbf{U}(t, t_0) \cdot \mathbf{z}(t_0), \end{aligned}$$

and  $\mathbf{D}\mathbf{F}(r) = \mathbf{D}\mathbf{F}[\mathbf{x}(r)]$ . Since the time evolution is stable (the system synchronizes)  $\mathbf{U}(t, t_0)$  shrinks  $\mathbf{z}(t_0)$  to zero exponentially fast as  $t \rightarrow \infty$ . The rate of decrease is controlled, in a nontrivial fashion, by the coupling,  $\epsilon$  [2,3,14].

Clearly,  $\mathbf{B}$  and  $\mathbf{A}$  are nontrivial functions of  $\epsilon$ . In addition,  $\mathbf{B}$  is a function of the type of noise in the driving signal (via the autocorrelation function of the noise) but is *not* a function of  $\sigma$  or the errors in modeling. On the other hand,  $\mathbf{A}$  is a function of modeling errors but is *not* a function of the noise. Indeed, one can use the numerical value of  $\mathbf{A}$  to obtain an order of magnitude estimate for the average errors in the modeling  $[\langle |\Delta \mathbf{G}|^2 \rangle]^{1/2}$  [3]. The scaling law given by Eqs. (7)–(9) indicates the effect of noise on the synchronization deviation level. Together, these equations answer the first question we asked in the introduction.

The second question asked in the introduction involved modeling errors and the effects of drift in the dynamics of the driving signal. Both of these effects influence  $\mathbf{A}$  while neither influences  $\mathbf{B}$ . Inserting Eq. (5) and the definition of  $\mathbf{H}(r)$  into Eq. (9) results in

$$\begin{aligned} A^2 &\simeq A'^2 \\ &+ \frac{\partial}{\partial \mathbf{p}} \left( \int_{t_0}^t \langle |\mathbf{U}(t, r) \cdot [\Delta \mathbf{G}'(r) + \mathbf{H}'(r)]|^2 \rangle dr \right) \cdot \delta \mathbf{p}, \end{aligned} \tag{10}$$

where  $\mathbf{H}'$  is what one obtains by substituting  $\Delta \mathbf{G}'$  for  $\Delta \mathbf{G}$  in the definition of  $\mathbf{H}$ , and  $A'^2$  is what one obtains by substituting  $\Delta \mathbf{G}'$  and  $\mathbf{H}'$  for  $\Delta \mathbf{G}$  and  $\mathbf{H}$  in Eq. (9). In the limit of zero noise the deviation level is just  $[\langle |z|^2 \rangle_T]^{1/2} = A$ , and Eq. (10) describes the rise of the deviation level as the dynamics of the driving drifts.

Numerical experiments addressing changes in the synchronization deviation level as a function of noise level,  $\sigma$ , and modeling errors,  $\Delta \mathbf{G}$ , were performed on data sets obtained from an electronic circuit. Details about the experimental apparatus that produced the scalar time series,  $s(n\Delta t) = s(n)$ ,  $n = 1, 2, \dots$  can be found in Ref. [3]. The time delay method

$$\mathbf{x}(n) = [s(n), s(n+T), \dots, s(n+(d-1)T)]$$

was used to reconstruct the attractors in a working phase space. The optimal time delays and embedding dimensions were determined using average mutual information and false near neighbors, respectively [3,15,16]. Global ODE models, in the form of Eq. (2), of the dynamics on the attractor were constructed using portions of the embedded time series [3,10].

Our first set of numerical experiments examined the behavior of  $[\langle |z|^2 \rangle_T]^{1/2}$  as a function of  $\sigma$ . Each numerical experiment used two types of noise. The first type is Gaussian noise with zero mean and unit standard deviation. The second type (inband noise) is constructed to have zero mean, unit standard deviation, and the same power spectrum as the raw time series. Two different values of the coupling constant were tested. One value was chosen slightly above the minimum necessary for synchronization while the second was chosen well above the minimum value. The numerical tests used 5000 point time averages.

The results of the tests are shown in Fig. 1 where we have plotted normalized deviation levels,  $[\langle |z|^2 \rangle_T]^{1/2}/D$ . The normalization constant,  $D$ , is the time average of  $|z|^2$  without coupling. The lines represent curves of best fit between Eq. (7) and the results of the numerical experiments.

## Electronic Circuit

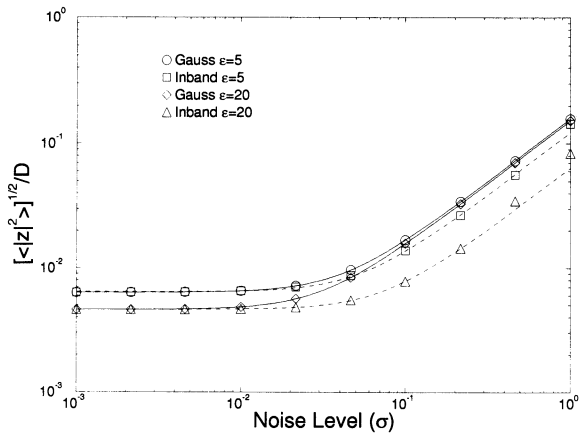


Fig. 1. The normalized synchronization levels as a function of added noise level. The circles and squares correspond to Gaussian and inband noise for  $\epsilon = 5$ . The diamonds and triangles correspond to Gaussian and inband noise for  $\epsilon = 20$ .

A second set of numerical experiments determined the behavior of the deviation level as a function of changes in the dynamics of the driving signal,  $\Delta G$ . In order to perform these tests we recorded six time series from the circuit each corresponding to a slightly different value of a parameter,  $\alpha_0, \dots, \alpha_5$  (physically, a resistance is changed in the circuit). A model, Eq. (2), was constructed from a portion of the  $\alpha_0$  time series and then subjected to driving from each time series. The measured deviation levels are shown in Fig. 2, where the solid lines represent straight lines of best fit through the data. The solid symbols indicate a linear rise in the deviation level with respect to changes in  $\alpha$  ( $|\Delta\alpha_j| = |\alpha_0 - \alpha_j|$ ).

The rise in the deviation level shown in Fig. 3 is due, predominantly, to changes in the dynamics of the driving signal [3]. If the amplitude of the noise is small then Eqs. (7), (9), and (10) imply that

$$\log_{10}\{\langle |z|^2 \rangle^{1/2}\} \simeq \log_{10}(A') + \frac{1}{2} \left( \frac{S}{A'} \right)^2 |\Delta\alpha|, \quad (11)$$

for suitably defined  $S(\epsilon)$  (see Eq. (10)). This equation explains the linear rise in the synchronization deviation level. The ability to track this rise is the center of a nondestructive testing application we discuss in our longer paper [3].

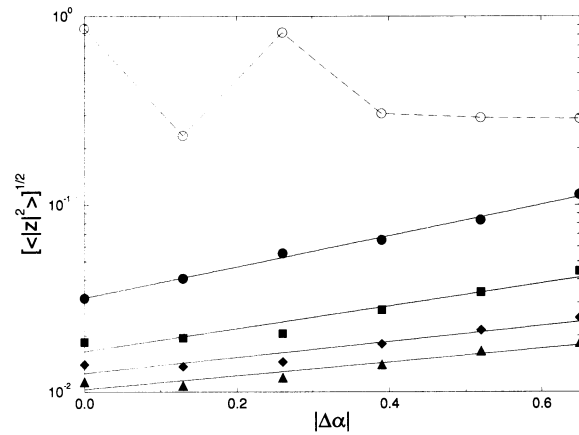


Fig. 2. The synchronization level as a function of  $\Delta\alpha$  and the coupling strength,  $\epsilon$ . The solid circles, squares, diamonds, and triangles represent  $\epsilon = 1, 2, 3$ , and 4, respectively. The open circles represent  $\epsilon = 0.5$  which is insufficient for synchronization. Each change in  $\Delta\alpha$  represents a change in the dynamics of the driving signal of approximately 1%.

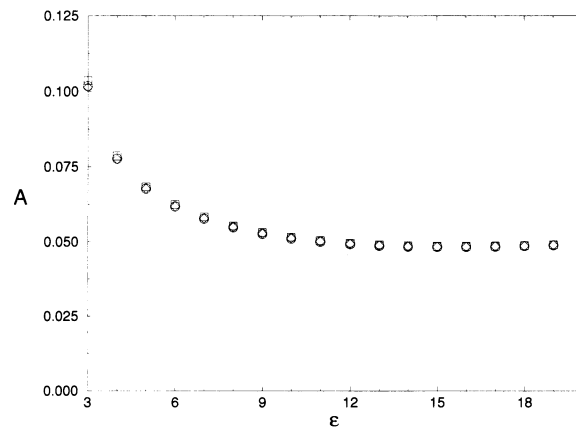


Fig. 3.  $A$  versus  $\epsilon$ .  $A$  has been calculated using raw data (diamonds) data with Gaussian noise (circles) and data with inband noise (squares).

Finally, we have investigated the functional dependence of  $A$  and  $B$  on the coupling strength  $\epsilon$ . Fig. 3 shows  $A$  versus  $\epsilon$  for three distinct cases. The first case (diamonds) used the raw data as the driving term in Eq. (3) and the approximation  $A^2 = \langle |z|^2 \rangle_T$ . The second two cases (circles and squares) used Gaussian and inband noise, respectively. To obtain  $A$  (as well as  $B$ ) for a particular value of  $\epsilon$  we calculated the deviation level as a function of noise size (see Fig. 1). We then fitted these results to Eq. (7) [17]. The fig-

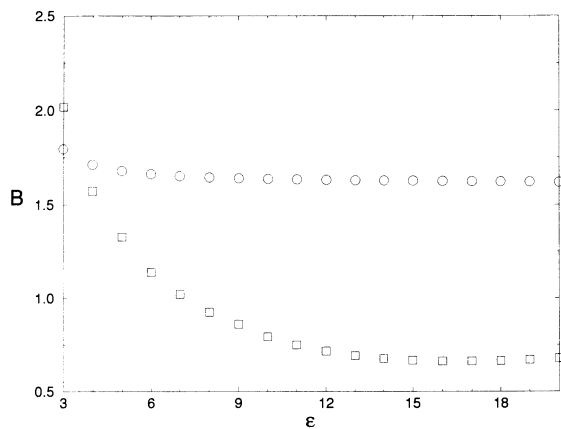


Fig. 4.  $B$  versus  $\epsilon$  for Gaussian (circles) and inband (squares) noise.

ure indicates that  $A$  is not a function of the type of noise in the driving.

Fig. 4 shows  $B$  versus  $\epsilon$  for inband and Gaussian noise. Quantitative details about the behavior of  $B$  depend intimately on the type of noise in the driving signal. An important special case is delta correlated noise where  $k(s) = k(0)\delta(s)$ . When the noise is delta correlated  $B = 0$  and it is possible to obtain a compact analytic expression for  $B^2$  [3]. The figures indicate that  $B$  is essentially independent of  $\epsilon$  for Gaussian noise and has a strong dependence on  $\epsilon$  for inband noise.

Figs. 3 and 4 show that both  $B$  and  $A$  appear to become independent of  $\epsilon$  when  $\epsilon$  gets large. This fact can be predicted since in the  $\epsilon \rightarrow \infty$  limit corresponds to Pecora and Carroll synchronization [1,3]. A partial theoretical analysis of the dependence of  $B$  and  $A$  on  $\epsilon$  can be found in Ref. [3].

N.F. Rulkov was supported by grant number DE-FG03-90ER14148 from the Department of Energy. N. Tuffillaro was supported by the Department of Energy.

## References

- [1] L.M. Pecora and T.L. Carroll, Phys. Rev. A 44 (1991) 2374.
- [2] J.F. Heagy, T.L. Carroll and L.M. Pecora, Phys. Rev. E 50 (1994) 1874.
- [3] R. Brown, N.F. Rulkov and N.B. Tuffillaro, Chaotic synchronization: The effects of additive noise and drift in the dynamics of the driving, Phys. Rev. E, in press.
- [4] H.D.I. Abarbanel, R. Brown, J.J. Sidorowich and L.S. Tsimring, Rev. Mod. Phys. 65 (1993) 1331.
- [5] K. Pyragas, Phys. Lett. A 170 (1992) 421.
- [6] D. Vassiliadis, Physica D 71 (1994) 319.
- [7] T.L. Carroll and L.M. Pecora, Physica D 67 (1993) 126.
- [8] K.M. Cuomo and A.V. Oppenheim, Phys. Rev. Lett. 71 (1993) 65.
- [9] A.R. Volkovskii and N.F. Rulkov, Tech. Phys. Lett. 19 (1993) 97.
- [10] R. Brown, N.F. Rulkov and E.R. Tracy, Phys. Rev. E 49 (1994) 3784.
- [11] T. Sauer, J.A. Yorke and M. Casdagli, J. Stat. Phys. 65 (1991) 579.
- [12] R. Brown, Orthonormal polynomials as prediction functions in arbitrary phase space dimensions, INLS preprint, April 1993.
- [13] T.C. Newell, P.M. Alsing, A. Gavrielides and V. Kovanis, Phys. Rev. E 49 (1994) 313.
- [14] H. Fujisaka and T. Yamada, Prog. Theor. Phys. 69 (1983) 32.
- [15] A.M. Fraser and H.L. Swinney, Phys. Rev. A 33 (1986) 1134; A.M. Fraser, IEEE Trans. Inf. Theory 35 (1989) 245.
- [16] M. Kennel, R. Brown and H.D. I. Abarbanel, Phys. Rev. A 45 (1992) 3403.
- [17] L. Ingber, Mathl. Comput. Modeling 8 (1993) 29.